Shiraz University

IJVR

ISSN: 1728-1997 (Print)
ISSN: 2252-0589 (Online)

Vol.25 No.2 Ser. No.87 2024

IRANIAN JOURNAL OF VETERINARY RESEARCH

Original Article

Ultrasonographic characterization of tendons and ligaments of palmar/plantar aspect of the cannon region in Egyptian donkeys

Gadallah, S.[1]; Sharshar, A.[2]; Fadel, M.[3]; Mahran, E.[4] and Hammad, A.[1*]

[1]Department of Surgery, Anesthesiology and Radiology, Faculty of Veterinary Medicine, University of Sadat City, Sadat City 32511, Egypt; [2]Department of Veterinary Clinical Sciences, Faculty of Veterinary Medicine, Jordan University of Science and Technology, Irbid 22110, Jordan; [3]Animal Reproduction Research Institute (ARRI)-Agricultural Research Center, Giza 12211, Egypt; [4]MSc Student, Animal Reproduction Research Institute (ARRI)-Agricultural Research Center, Giza 12211, Egypt

[*]***Correspondence:*** *A. Hammad, Department of Surgery, Anesthesiology and Radiology, Faculty of Veterinary Medicine, University of Sadat City, Sadat City 32511, Egypt. E-mail: amal.abdelhakam@vet.usc.edu.eg*

10.22099/IJVR.2024.47480.6859

(Received 25 May 2023; revised version 17 May 2024; accepted 16 Jun 2024)

Abstract

Background: There is a scarcity of data regarding the ultrasonographic characterization of tendons and ligaments in the distal limbs of donkeys. **Aims:** To determine ultrasonographic characteristics of normal tendons and ligaments at the palmar/plantar aspect of the cannon region in Egyptian donkeys. **Methods:** B-mode ultrasonography was conducted for the proposed tendons and ligaments in 12 clinically normal donkeys. Targeted structures were examined using transverse and longitudinal scans and evaluated in shape, echogenicity, echogenic pattern, fiber alignment pattern, and cross-sectional area (CSA). **Results:** Using transverse scan, the sonographic shapes of tendons and ligaments of metacarpal and metatarsal regions were determined. Upon examining different levels of each region, specific ligaments, not tendons, were present only at the higher levels. The echogenicity of ligaments and tendons was either similar or variable across different levels. All tendons and ligaments displayed homogeneous echogenicity except for the suspensory ligament. In the longitudinal scan, tendons maintained linear and parallel fiber alignment along examination levels. Conversely, ligaments displayed mostly inconstant fiber patterns (linear/crimp). There was a statistically significant ($P<0.05$) difference in CSA of tendons and ligaments between certain levels within metacarpal and metatarsal regions. Upon comparing metacarpal and metatarsal regions, there were distinct variations in some ultrasonographic characteristics of the same tendons and ligaments. **Conclusion:** This study established the ultrasonographic features of normal tendons and ligaments at the palmar/plantar aspect of the cannon region in donkeys (*Equus asinus*). These ultrasonographic data can be a reference guide when cannon region lameness is suspected.

Key words: Cannon region, Donkey, Ligaments, Tendons, Ultrasonography

Introduction

Donkeys are used for labor in developing countries, particularly in Egypt, despite increasing mechanization worldwide (Uerpmann, 1991). However, there is a significant occurrence of lameness in these animals, which has a detrimental effect on their well-being and working capability (Pritchard *et al*., 2005; Abdel-Hady *et al*., 2017; Assefa *et al*., 2017). Lameness in these working animals typically arises from injuries to various tissues in the lower limb, such as bone, joints, tendons, and ligaments (Usman *et al*., 2015; Abdel-Hady *et al*., 2017; Assefa *et al*., 2017).

Imaging techniques yield important pathologic and physiologic information and give a clearer image, allowing rapid and more precise diagnosis for different conditions. Various imaging modalities, including computed tomography (CT), magnetic resonance imaging (MRI), and ultrasonography, have been developed to aid in the diagnosis of tendon and ligament injuries. CT and MRI require general anesthesia of the examined animals. However, the associated expenses pose a significant financial burden for the owner, limiting their extensive utilization under field conditions (Pilsworth and Head, 2010).

Conversely, ultrasonography is widely acknowledged as a routine, non-invasive diagnostic technique that provides detailed information about soft tissue injuries (Denoix *et al*., 1992; Denoix, 1994; Reef, 1998; Pickersgill *et al*., 2001; Rantanen *et al*., 2003). The evaluation of tendons and ligaments in the metacarpal and pastern regions is commonly performed using this

imaging modality. It is also the most frequently used method for examining the suspensory apparatus of horses (Rheimer, 2010; Carnicer *et al*., 2013). Ultrasonography was also effective in setting the normal cross-sectional area of tarsal ligaments in Standardbred horses as well as in identifying the alterations in palmar and plantar tendons and ligaments of the metacarpal and metatarsal regions in unused gaited horses (Spinella *et al*., 2018; Schade *et al*., 2021).

Donkeys are widely play a crucial role in serving humans; nevertheless, they have not received the same attention level compared to horses in treating injuries. In this regard, few attempts have been characterized the nature of lameness in donkeys (Abdel-Hady *et al*., 2017; Assefa *et al*., 2017).

Ultrasonography, CT, and MRI have been previously assessed as non-invasive diagnostic imaging tools for donkeys. These diagnostic modalities effectively evaluated digit and carpal joints in donkeys and set a reference database for the imaged structures (Salem *et al*., 2019; Salem *et al*., 2022). Ultrasonography was successful in imaging tendons and ligaments of the palmar/plantar aspect of the cannon region in donkeys (Nazem *et al*., 2015; Parés-Casanova and Junquera-Muñoz, 2021). However, the current data on the ultrasonographic assessment and characterization of tendons and ligaments in donkey limbs, specifically in the cannon region, is either limited or insufficient (considering the cannon region in donkeys).

Therefore, this study aimed to determine ultrasonographic characteristics of normal tendons and ligaments at the palmar/plantar aspect of the cannon region in donkeys (*Equus asinus*). We hypothesized that some variations would be present in ultrasonographic characteristics of the scanned tendons and ligaments of palmar and plantar cannon regions or possibly in between.

Materials and Methods

This study was conducted at the Hospital of Surgery, Anesthesiology and Radiology Department, Faculty of Veterinary Medicine, University of Sadat City, Egypt.

Animals

The study included 12 clinically normal donkeys (Equus asinus/drafting donkeys) of both sexes (9 intact males and three non-pregnant females) weighing between 150-190 kg and aged 7-10 years. The studied animals exhibited no musculoskeletal disorders (based on physical examination and lameness scoring). Additionally, their body condition scores fell within the range of 3-4. During the study period, donkeys were housed in separate stalls and fed hay during the daytime and 1 kg concentrate at night, with free access to water. This study was approved by the Institutional Animal Care and Use Committee of the Faculty of Veterinary Medicine, University of Sadat City, Egypt (protocol No.: VUSC-028-1-21). The studied animals were owned by the institution and used for teaching purposes.

Study design

All animals' tendons and ligaments at the palmar/plantar aspect of the cannon region were examined using B-mode ultrasonography. We utilized an ultrasound system (EsaoteMyLab™One VET, Italy) equipped with a 10-18 MHz linear array transducer and a built-in caliper system.

Before scanning, the palmar/plantar area from the accessory carpal bone in the forelimb and the point of hock in the pelvic limb down to the proximal sesamoid bones were prepared by clipping and shaving the hair. The skin was thoroughly washed with water and degreased by ethyl alcohol 70%. The ultrasound coupling gel was applied to the entire area being scanned. In order to facilitate the preparation of the targeted areas, the studied animals were restrained in a stanchion and sedated using xylazine hydrochloride (Xyla-Ject® 20 mg/ml, Adwia Co., Egypt) at a dose of 1.1 mg/kg, IV (Hall *et al*., 2001).

Each palmar metacarpal and the plantar metatarsal region was divided into seven examination levels labeled 1A, 1B, 2A, 2B, 3A, 3B, and 3C. The examination levels were equidistant, measuring 2.5-3 cm, starting 4 cm distal to the accessory carpal bone and the point of the hock in fore and hind limbs, respectively, till the level of the proximal sesamoid bone at the fetlock joint for both

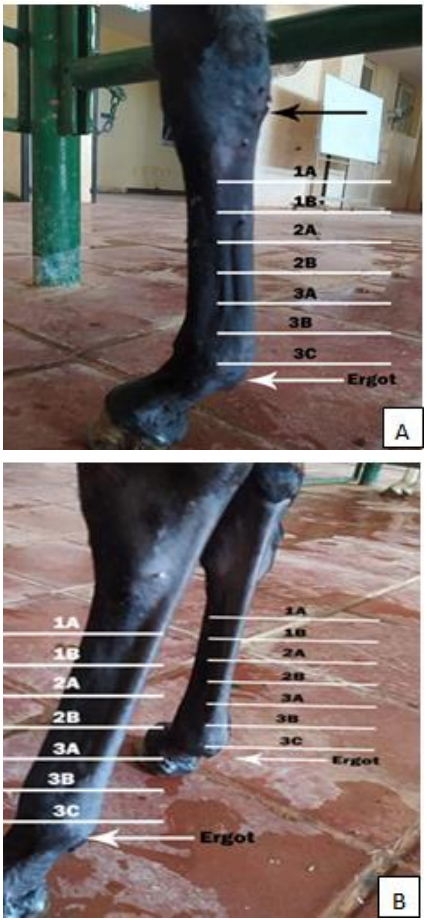

Fig. 1: Different levels of scanning at metacarpal (**A**), and metatarsal regions (**B**)

fore and hind limbs (Nazem *et al*., 2015; Parés-Casanova and Junquera-Muñoz, 2021) (Fig. 1).

All levels were scanned in longitudinal and transverse plans by progressive movement of the probe from the proximal to the distal limit of the targeted area. Another plantaromedial scan was also performed during an examination of level 1A of the pelvic limb for a complete examination of different structures. During the scanning procedure, animals stood squarely on a flat floor with weight equally distributed on the four limbs (Kimberly and Kidd, 2014). Excessive pressure on the probe was avoided to prevent any changes in the shape and size of the underlying structures. The frequency, depth, and incident angle were adjusted during the examination to obtain high-quality images for the scanned structures. Throughout the whole study, scanning was performed by the same sonographer.

Assessments

At the examination levels, the tendons and ligaments at palmar metacarpal and plantar metatarsal regions of contra fore and hind limbs were evaluated in terms of shape, echogenicity, echogenic pattern, fiber alignment pattern, and cross-sectional area (CSA). The built-in software of the ultrasound machine was used to measure the cross-sectional area of the targeted structures.

Statistical analysis

The sample size calculation for reliable analysis was performed using Andrew Fisher's formula, which suggested a study size of 12 donkeys to achieve a confidence level of 80%. Statistical analysis was performed using SPSS 20.0 software (SPSS Inc., Chicago, IL, USA). The CSA of tendons and ligaments at palmar metacarpal and plantar metatarsal regions were analyzed using a One-way analysis of variance (ANOVA). Tukey's test was used to compare the CSA of the same structure among all examination levels of the same limb and at each level among metacarpal and metatarsal regions. Results were expressed as a mean±SD. The level of significance was set at $P<0.05$.

Results

Metacarpal region

In the transverse scan of levels 1A and 1B, skin and subcutis appeared as echogenic layers. Directly underneath, the superficial digital flexor tendon (SDFT) was imaged as an hourglass-shaped echogenic structure. Dorsal to SDFT, deep digital flexor tendon (DDFT) was visualized as a pear-shaped echogenic structure. Dorsal to DDFT, the inferior check ligament (ICL) appeared as an irregular coma-shaped echogenic structure at level 1A and an irregular rectangular shape at level 1B. The suspensory ligament (SL) appeared as a rectangular-shaped echogenic structure at the palmar aspect of MCIII (hyperechoic line). Dorsal to SDFT and dorsomedial to DDFT, at levels 1A and 1B, an echogenic structure of approximately an hourglass shape was imaged. This structure was termed the Accessory Inferior Ligament of SDFT (AIL-SDFT). Only at level 1A, at the palmar aspect of SDFT, the carpal retinaculum was imaged as a thin hyperechoic line (Figs. 2 and 3).

At both examination levels, SDFT, DDFT, AIL-SDFT, and ICL were of homogeneous echogenicity, while SL was heterogeneous (slightly less at level 1B

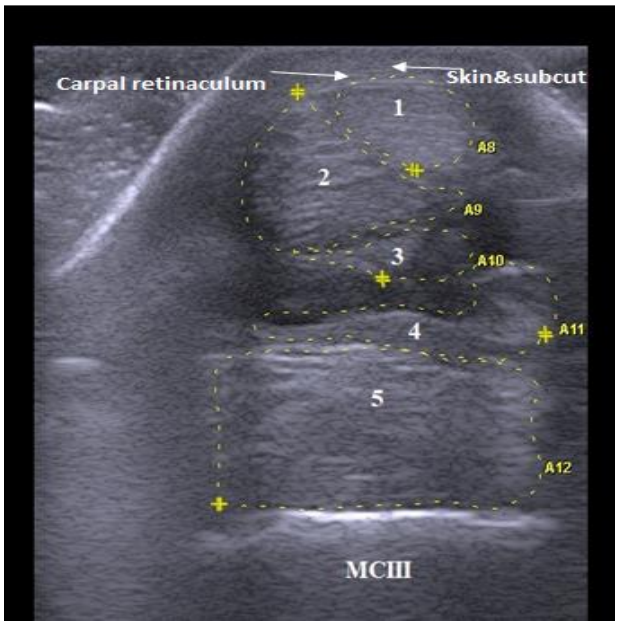

Fig. 2: Transverse ultrasonographic scan of palmar metacarpal region at level 1A showing: (**1**) SDFT (superficial digital flexor tendon), (**2**) DDFT (deep digital flexor tendon), (**3**) AIL-SDFT (accessory inferior ligament of superficial digital flexor tendon), (**4**) ICL (inferior check ligament), and (**5**) SL (suspensory ligament). MCIII (third metacarpal bone)

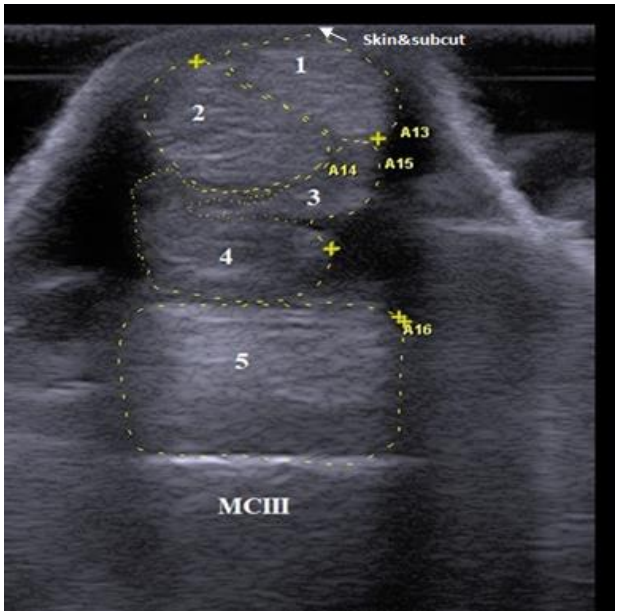

Fig. 3: Transverse ultrasonographic scan of palmar metacarpal region at level 1B showing: (**1**) SDFT (superficial digital flexor tendon), (**2**) DDFT (deep digital flexor tendon), (**3**) AIL-SDFT (accessory inferior ligament of superficial digital flexor tendon), (**4**) ICL (inferior check ligament), and (**5**) SL (suspensory ligament). MCIII (third metacarpal bone)

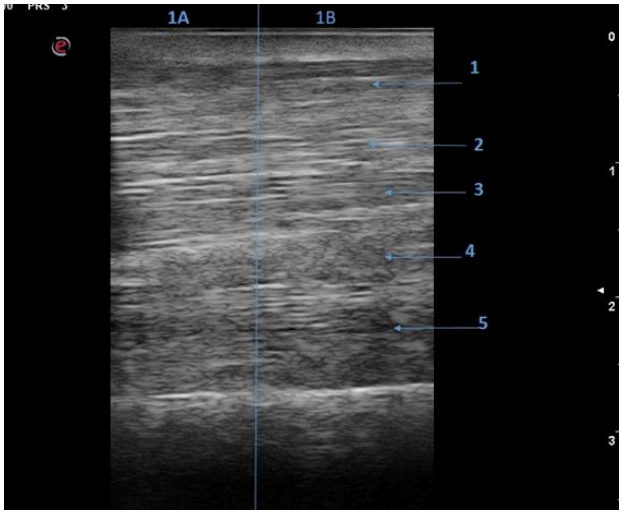

Fig. 4: Longitudinal ultrasonographic scan of palmar metacarpal region at levels 1A and 1B showing: (**1**) SDFT (superficial digital flexor tendon), (**2**) DDFT (deep digital flexor tendon), (**3**) AIL-SDFT (accessory inferior ligament of superficial digital flexor tendon), (**4**) ICL (inferior check ligament), and (**5**) SL (suspensory ligament)

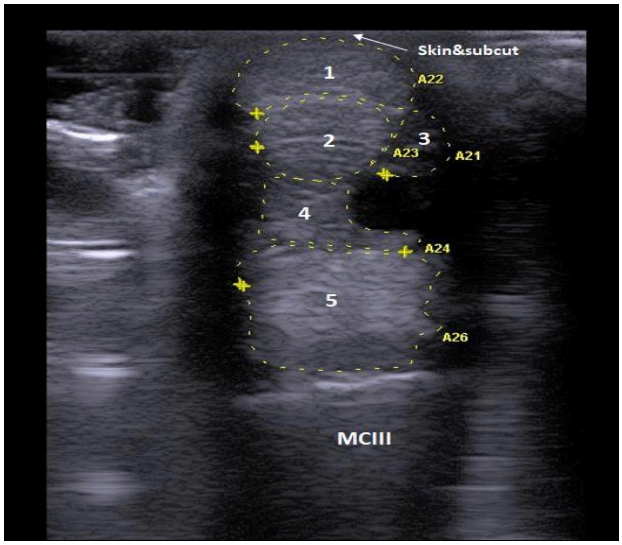

Fig. 5: Transverse ultrasonographic scan of palmar metacarpal region at level 2A showing: (**1**) SDFT (superficial digital flexor tendon), (**2**) DDFT (deep digital flexor tendon), (**3**) AIL-SDFT (accessory inferior ligament of superficial digital flexor tendon), (**4**) ICL (inferior check ligament), and (**5**) SL (suspensory ligament). MCIII (third metacarpal bone)

relative to level 1A). At levels 1A and 1B, SL was hyperechoic to other soft structures. DDFT and SDFT were nearly isoechoic while being slightly hyperechoic to both ICL and AIL-SDFT (Figs. 2 and 3). In the longitudinal scan of levels 1A and 1B, all of the examined structures (SDFT, DDFT, ICL, SL, and AIL-SDFT) appeared to have a uniform linear fiber alignment parallel to the longitudinal axis of MCIII with coarser linear fiber for SL (Fig. 4).

In the transverse scan of levels 2A and 2B, SDFT appeared as a kidney-shaped structure (thicker at midline), while the DDFT appeared as an ovoid-shaped

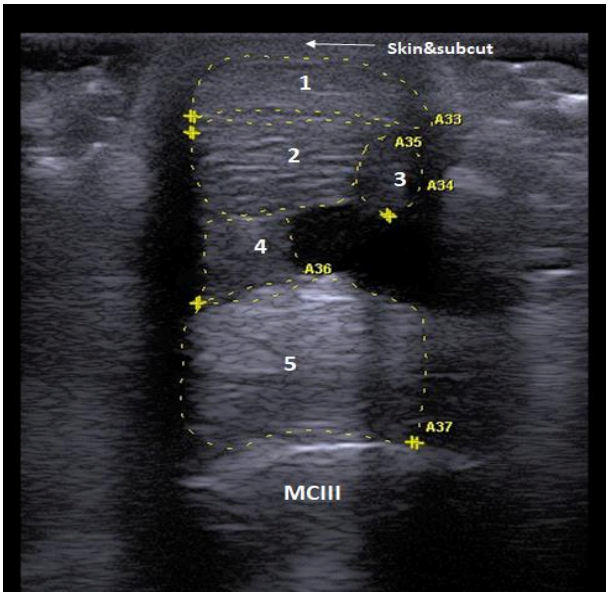

Fig. 6: Transverse ultrasonographic scan of palmar metacarpal region at level 2B showing: (**1**) SDFT (superficial digital flexor tendon), (**2**) DDFT (deep digital flexor tendon), (**3**) AIL-SDFT (accessory inferior ligament of superficial digital flexor tendon), (**4**) ICL (inferior check ligament), and (**5**) SL (suspensory ligament). MCIII (third metacarpal bone)

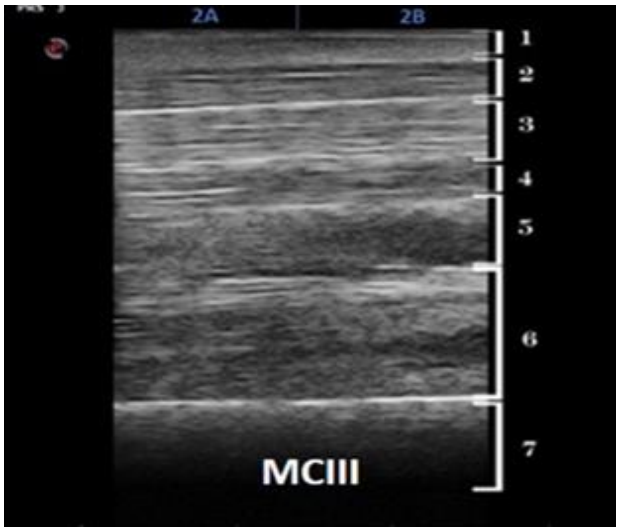

Fig. 7: Longitudinal ultrasonographic scan of palmar metacarpal region at levels 2A-2B showing: (**1**) skin and subcutaneous, (**2**) SDFT (superficial digital flexor tendon), (**3**) DDFT (deep digital flexor tendon), (4) AIL-SDFT (accessory inferior ligament of superficial digital flexor tendon), (**5**) ICL (inferior check ligament), and (**6**) SL (suspensory ligament). MCIII (third metacarpal bone)

structure (more regular at level 2A). SL and AIL-SDFT showed no changes at both levels compared to the more proximate levels (1A and 1B). The ICL appeared as an irregularly shaped rectangular structure between DDFT and SL at level 2A. However, at level 2B, it was of a more regular rectangular shape. Regarding echogenicity, SL was the most echogenic structure, followed by DDFT and AIL-SDFT (both showed nearly the same echogenicity), ICL, and SDFT. All structures other than

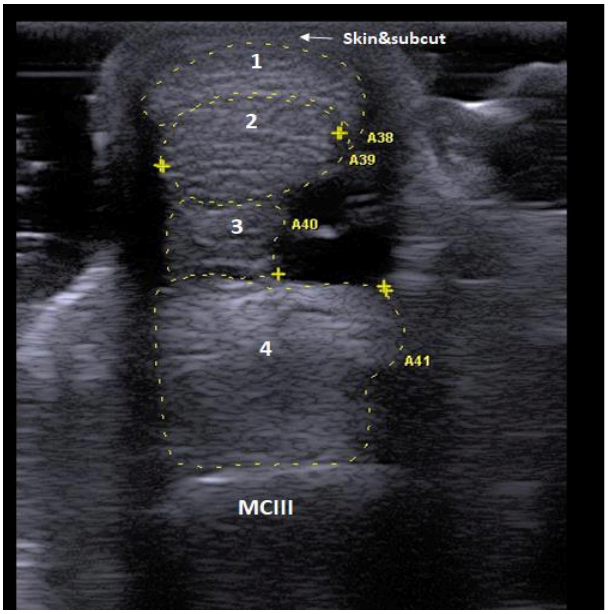

Fig. 8: Transverse ultrasonographic scan of palmar metacarpal region at level 3A showing: (**1**) SDFT (superficial digital flexor tendon), (**2**) DDFT (deep digital flexor tendon), (**3**) ICL (inferior check ligament), and (**4**) SL (suspensory ligament). MCIII (third metacarpal bone)

SL (heterogeneous; slightly less at level 2A than levels 1B and 2B) displayed homogeneous echogenicity (Figs. 5 and 6). During the longitudinal scan of these levels, the SDFT and DDFT exhibited linear fiber alignment, whereas SL presented some coarse fibers predominantly of crimp pattern (waving pattern). At level 2A, AIL-SDFT and ICL showed different fiber characteristics. Unlike ICL, some fibers presented linear fiber alignment. However, at level 2B, both structures had a definite fiber pattern (Fig. 7).

In the transverse scan of level 3A, SDFT appeared as a semilunar-shaped structure engulfing the palmar aspect of DDFT that exhibited an ovoid shape. Both ICL and SL maintained their rectangular shape. The echogenicity showed no changes compared to the more proximate levels (2A and 2B). In terms of the echogenic pattern, all structures exhibited homogeneous echogenicity, unlike SL (slightly less heterogenic compared to the preceding level). At this level, AIL-SDFT no longer exists (Fig. 8). At level 3B, SDFT appeared as a flattened semilunar-shaped structure encircling DDFT with manica flexoria that appeared as a homogeneous echogenic structure. The DDFT had an ovoid shape, whereas the SL had a butterfly-like shape, dividing into lateral and medial branches, with the medial branch being slightly larger than the lateral branch. SDFT, DDFT, and SL were relatively isoechoic. In contrast to the preceding level, ICL was no longer discernable at the current level. The echogenic pattern of all structures, except for SL, remained unchanged compared to the preceding level (Fig. 9).

Longitudinal scanning of levels 3A and 3B showed the linear fiber alignment pattern of SDFT and DDFT and the crimp pattern (slight) of SL fibers. At level 3A,

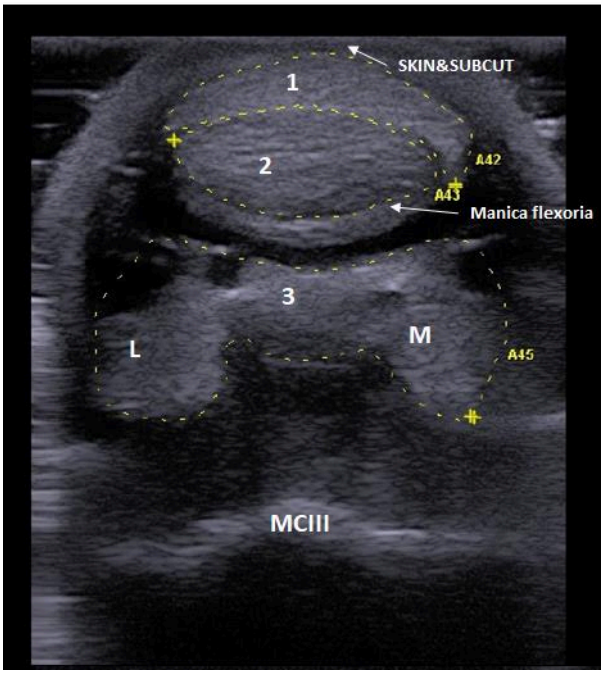

Fig. 9: Transverse ultrasonographic scan of palmar metacarpal region at level 3B showing: (**1**) SDFT (superficial digital flexor tendon), (**2**) DDFT (deep digital flexor tendon), (**3**) SL (suspensory ligament: M: Medial branch, and L: Lateral branch)

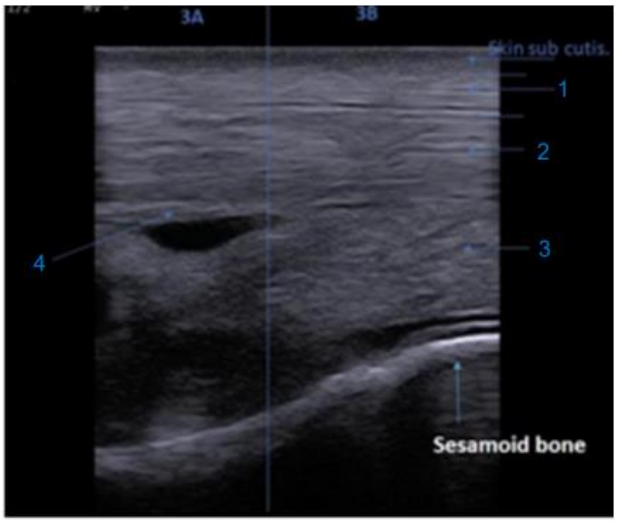

Fig. 10: Longitudinal ultrasonographic scan of palmar metacarpal region at levels 3A and 3B showing: (**1**) SDFT, (**2**) DDFT, (**3**) SL, and (**4**) ICL (3A)

the ICL fibers showed a minor crimp pattern. However, at level 3B, it was no further discernable as a single structure as it fused to DDFT, and both were imaged as one structure. Furthermore, at level 3B, manica flexoria was imaged as a hyperechoic band dorsal to DDFT (Fig. 10).

During the transverse scan of level 3C, the palmar annular ligament appeared as a hyperechoic line at the palmar aspect of SDFT. The SDFT had a semilunar shape and encircled the DDFT with the manica flexoria, imaged as a hyperechoic line extending around the

DDFT. The latter appeared as an elliptical structure. Both SDFT and DDFT appeared isoechoic, exhibiting similar echogenicity. Additionally, at this level, intersesamoidean ligament was evident as a homogeneous echogenic structure (with approximately equal echogenicity to DDFT and SDFT) occupying the space between sesamoid bones. It also extended beyond their margins (Fig. 11). In the longitudinal scan of this level, directly beneath the skin and subcutis, the palmar annular ligament was imaged as a hyperechoic line extending along the palmar aspect of SDFT. Dorsal to SDFT, manica flexoria was imaged as a thin hyperechoic line at the palmar aspect of the DDFT and even its dorsal aspect. Both SDFT and DDFT exhibited linear fiber alignment. The intersesamoidean ligament was imaged at this scan, showing crimp fibers perpendicular to those of the SDFT and DDFT (Fig. 12).

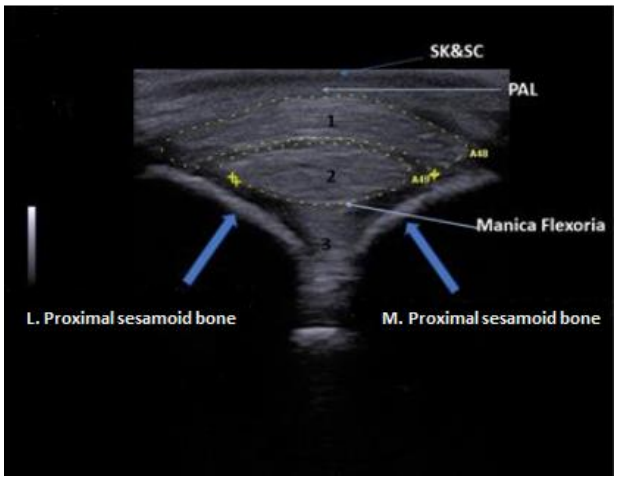

Fig. 11: Transverse ultrasonographic scan of palmar metacarpal region at level 3C showing: (**1**) SDFT (superficial digital flexor tendon), (**2**) DDFT (deep digital flexor tendon), (**3**) Intersesamoidean ligament, and PAL: Palmar annular ligament

Fig. 12: Longitudinal ultrasonographic scan of palmar metacarpal region at level 3 showing: SDF: Superficial digital flexor tendon, DDF: Deep digital flexor tendon, and PAL: Palmar annular ligament

Metatarsal region

The transverse scan of levels 1A and 1B revealed that SDFT appeared as a structure with an hourglass shape, tapering at one end and deviating towards either the medial side (1A) or the lateral side (1B) of the longitudinal axis of the MTIII. At these levels, DDFT appeared as a cup-shaped echogenic structure engulfing SDFT (projecting more laterally than medially) at level 1A. In contrast, at level 1B, it appeared as a circular-shaped structure. SL exhibited a nearly rectangular shape at levels 1A and 1B. ICL was scanned as a rectangular structure at levels 1A and 1B. The plantar ligament was clearly visible as an echogenic structure at the lateral side of SL (at level 1A) and close to the margin of ICL at level 1B. Regarding the echogenicity of the examined structures, at level 1A, both SDFT and DDFT were isoechoic to each other and slightly hyperechoic to ICL, while SL was the least echogenic structure. At level 1B, SL was the most echogenic structure, followed by ICL, SDFT, and DDFT (both displayed comparable echogenicity to each other). All tendinous and ligamentous structures were of homogeneous echogenicity, except for SL, which was slightly heterogenicity (less heterogeneous at level 1B than level 1A) (Figs. 13 and 14).

The longitudinal scan of levels 1A and 1B, SDFT, and DDFT exhibited linear fiber alignment (parallel to the long axis of MTIII). The tarsal sheath was also evident as a hyperechoic line at the plantar and dorsal margins of DDFT. Dorsal to DDFT, ICL was evident with predominately longitudinally aligned linear fibers (some fibers exhibited crimp pattern). Dorsal to ICL, SL was imaged, and some of its fibers displayed a crimp pattern. The plantar ligament was imaged at the plantar

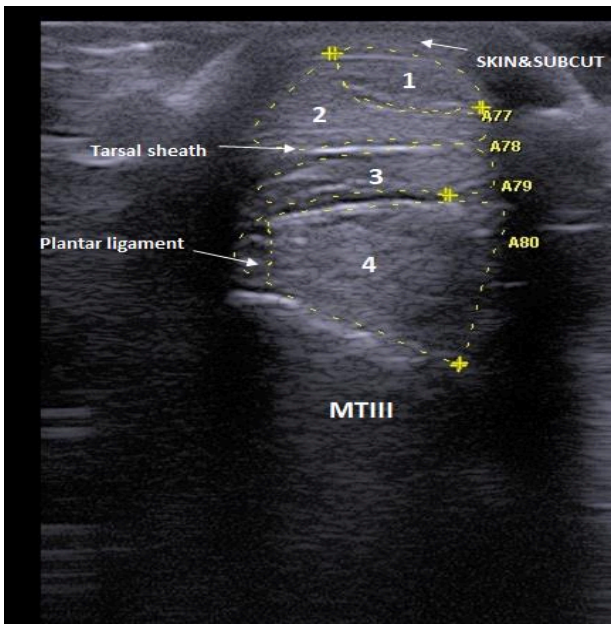

Fig. 13: Transverse ultrasonographic scan of plantar metatarsal region at level 1A showing: (**1**) SDFT (superficial digital flexor tendon), (**2**) DDFT (deep digital flexor tendon), (**3**) ICL (inferior check ligament), and (**4**) SL (suspensory ligament). MTIII (third metatarsal bone)

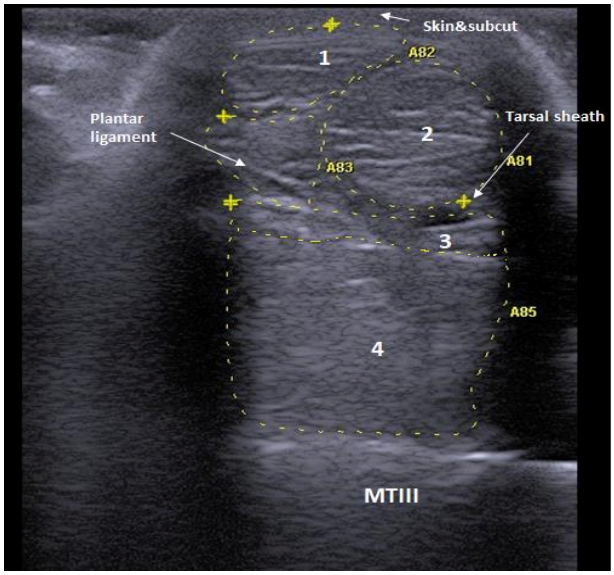

Fig. 14: Transverse ultrasonographic scan of plantar metatarsal region at level 1B showing: (**1**) SDFT (superficial digital flexor tendon), (**2**) DDFT (deep digital flexor tendon), (**3**) ICL (inferior check ligament), and (**4**) SL (suspensory ligament). MTIII (third metatarsal bone)

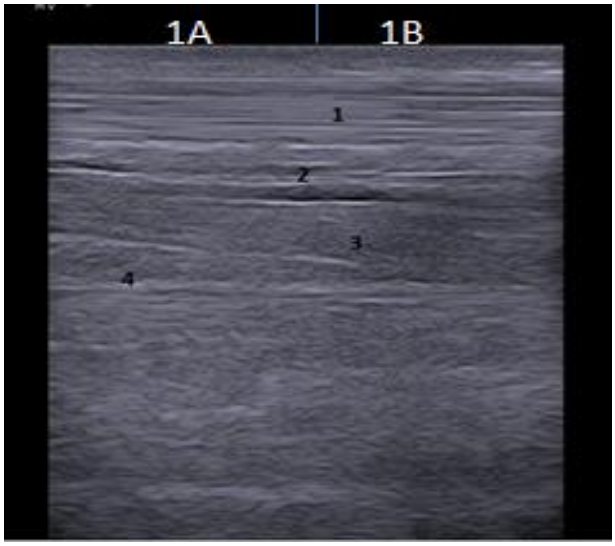

Fig. 15: Longitudinal ultrasonographic scan of plantar metatarsal region at levels 1A and 1B showing: (**1**) SDFT (superficial digital flexor tendon), (**2**) DDFT (deep digital flexor tendon), (**3**) ICL (inferior check ligament), (**4**) Plantar Ligament, and (**5**) SL (suspensory ligament)

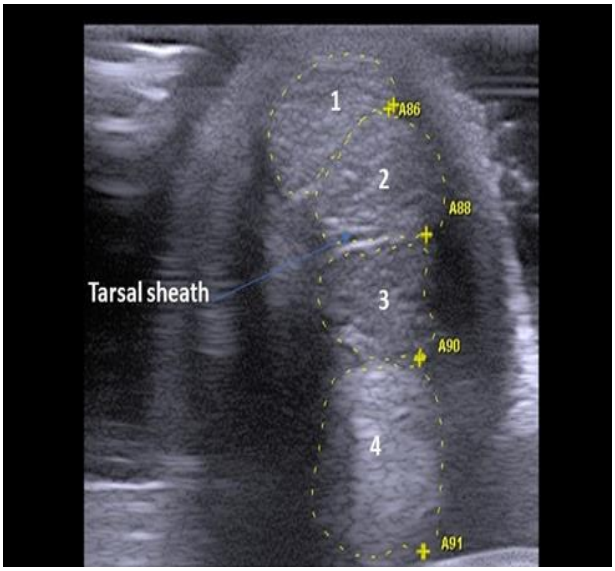

Fig. 16: Transverse ultrasonographic scan of plantar metatarsal region at level 2A showing: (**1**) SDFT (superficial digital flexor tendon), (**2**) DDFT (deep digital flexor tendon), (**3**) ICL (inferior check ligament), and (**4**) SL (suspensory ligament)

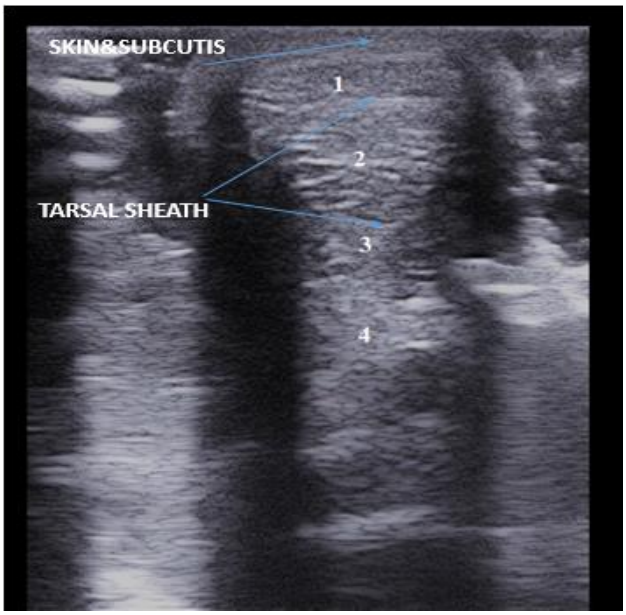

Fig. 17: Transverse ultrasonographic scan of plantar metatarsal region at level 2B showing: (**1**) SDFT (superficial digital flexor tendon), (**2**) DDFT (deep digital flexor tendon), (**3**) ICL (inferior check ligament), and (**4**) SL (suspensory ligament)

margin of SL, and its fibers exhibited a crimp pattern. At level 1B, the plantar ligament was only partially visible, appearing only at the proximal portion of this level, in contrast to level 1A (Fig. 15).

The transverse scan of levels 2A and 2B revealed different sonographic shapes for the SDFT and DDFT. At level 2A, SDFT exhibited an hourglass shape, while at level 2B appeared kidney-shaped. DDFT appeared as an ovoid-shaped structure at levels 2A and 2B. SL and ICL showed the same ultrasonographic shape as level 1B. The plantar ligament was absent at these levels. At level 2A, SL was the most echogenic structure, followed by SDFT and DDFT (they were isoechoic to each other), while ICL showed the least. At level 2A, the SL exhibited the highest echogenicity, followed by the SDFT and DDFT (which had the same echogenicity as each other), while the ICL displayed the lowest echogenicity. At these levels, the echogenic pattern of all examined structures was similar to that of the most proximate levels (1A and 1B) (Figs. 16 and 17). Longitudinal scanning of level 2A revealed fiber alignment patterns of different structures comparable to those of the previous levels. However, there was an absence of the plantar ligament and the fiber alignment

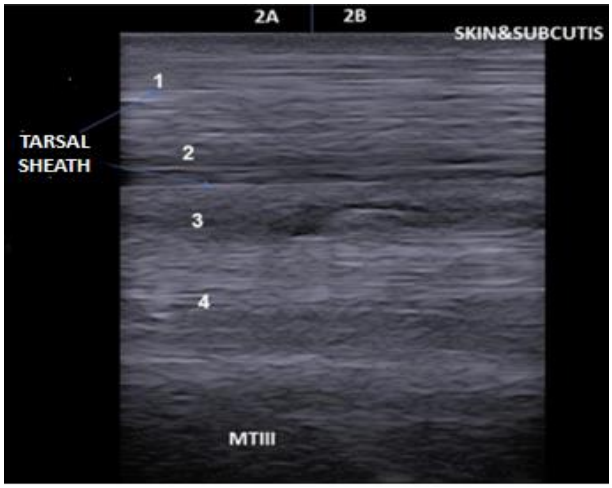

Fig. 18: Longitudinal ultrasonographic scan of plantar metatarsal region at levels 2A and 2B showing: (**1**) SDFT (superficial digital flexor tendon), (**2**) DDFT (deep digital flexor tendon), (**3**) ICL (inferior check ligament), and (**4**) SL (suspensory ligament)

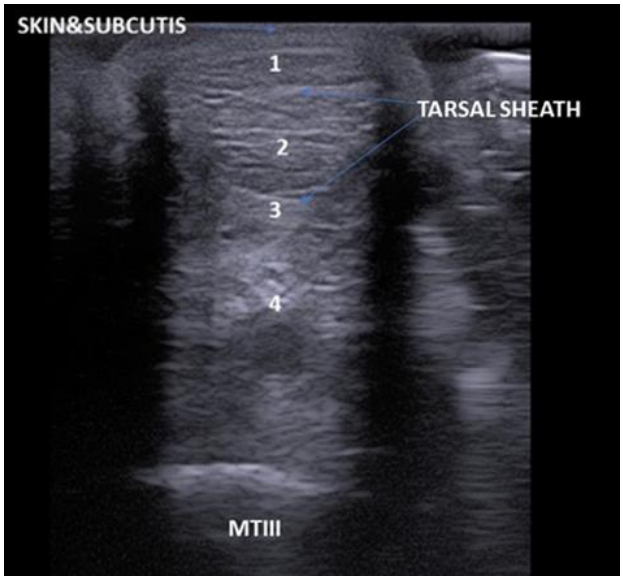

Fig. 19: Transverse ultrasonographic scan of plantar metatarsal region at level 3A showing: (**1**) SDFT (superficial digital flexor tendon), (**2**) DDFT (deep digital flexor tendon), (**3**) ICL (inferior check ligament), and (**4**) SL (suspensory ligament). MTIII (third metatarsal bone)

of ICL (slight presentation of waving pattern without any longitudinally aligned linear fibers). At level 2B, the longitudinal sonogram closely resembled the previous level, with only minor differences in the thickness of different structures and rare presentation of crimp patterns across SL and ICL (Fig. 18).

In the transverse scan of level 3A, all examined structures showed the same ultrasonographic shape and echogenic pattern as the preceding level. The echogenicity among different structures varied in this level relative to the preceding one. SDFT and DDFT were nearly isoechoic to each other and slightly less echogenic compared to ICL and SL (SL was of higher echogenicity than ICL) (Fig. 19). The transverse scan of

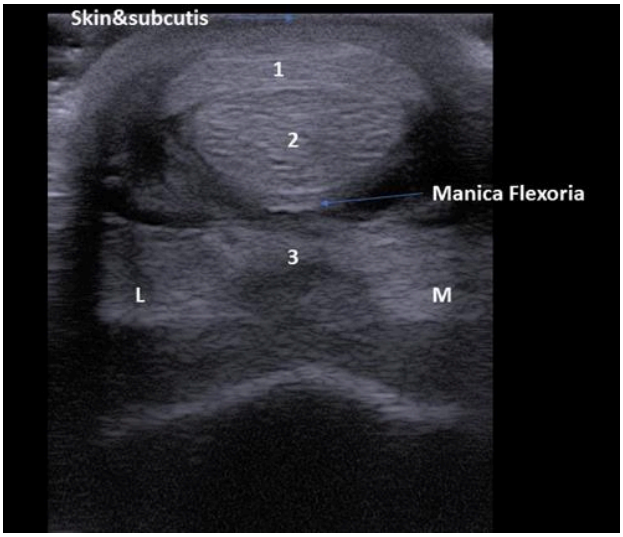

Fig. 20: Transverse ultrasonographic scan of plantar metatarsal region at level 3B showing: (**1**) SDFT (superficial digital flexor tendon), (**2**) DDFT (deep digital flexor tendon), and (**3**) SL (suspensory ligament)

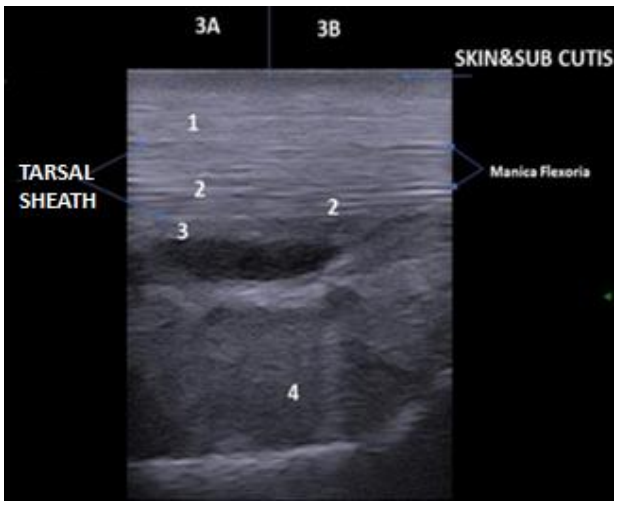

Fig. 21: Longitudinal ultrasonographic scan of plantar metatarsal region at level 3A and 3B shwoing: (**1**) SDFT (superficial digital flexor tendon), (**2**) DDFT (deep digital flexor tendon), and (**3**) SL (suspensory ligament)

the subsequent level (level 3B) was almost similar to the corresponding one in the forelimb. At this level, ICL was absent, and DDFT was surrounded by manica flexoria, which was imaged as a hyperechoic band (Fig. 20). The longitudinal sonogram of level 3A was similar to that of level 2B. Conversely, at level 3B, the examined structures exhibited identical longitudinal ultrasonographic picture as the more proximate levels (2B and 3A) except for the absence of tarsal sheath and ICL, which were no longer evident as a single structure, and the presence of manica flexoria. Upon comparing it with the corresponding level in the forelimb, it was observed that this level exhibited a high degree of similarity, except for the rare presentation of a crimp pattern of fiber alignment across the SL (Fig. 21).

The transverse scan of level 3C resembled the shape and arrangement of various structures to the

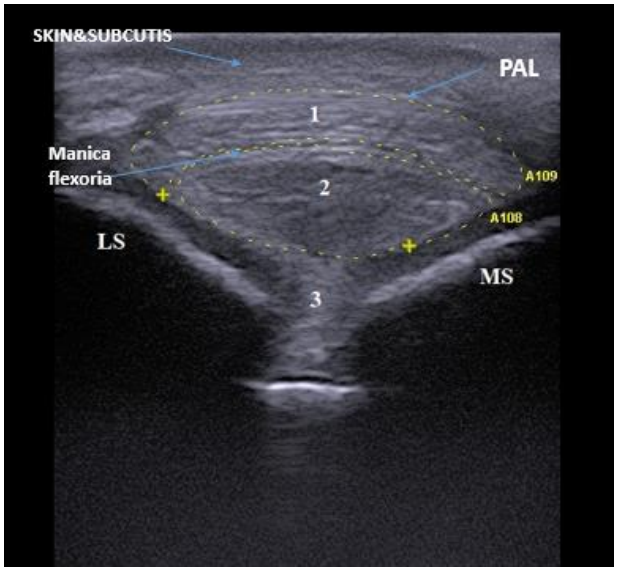

Fig. 22: Transverse ultrasonographic scan of plantar metatarsal region at level 3C showing: (**1**) SDFT (superficial digital flexor tendon), (**2**) DDFT (deep digital flexor tendon), (**3**) Inter-sesamoidean ligament, LS: Lateral sesamoid bone, and MS: Medial sesamoid bone

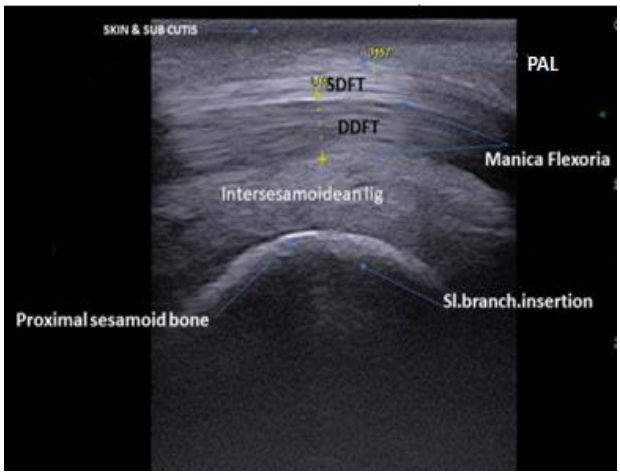

Fig. 23: Longitudinal ultrasonographic scan of plantar metatarsal region at level 3C showing: SDFT (superficial digital flexor tendon), DDFT (deep digital flexor tendon), and PAL: Plantar annular ligament

corresponding level in the forelimb. However, it was observed that the SDFT and DDFT were larger than the forelimb (Fig. 22). When comparing the hind limb to the previous level, specific structures showed changes in both shape (DDFT) and size (SDFT and DDFT), as well as the presence of the intersesamoidean ligament. Longitudinal scans at this level resembled the corresponding scans in the fore limb except for the nomenclature of the annular ligaments, as the plantar annular ligament was named in the hind limb. Conversely, there were some differences in this scan compared to the preceding one of the metatarsal region (Fig. 23).

Table 1 shows significant differences in the CSA of tendons and ligaments at specific levels within the metacarpal and metatarsal regions. Additionally, the greatest CSA of SDFT was found at level 3C in both the metacarpal and metatarsal regions. Also, the greatest CSA of DDFT for both regions was found at level 3B. The CSA of SL was greatest at levels 3B and 3A for the metacarpal and metatarsal regions, respectively. The CSA of ICL was greatest at level 1B for the metacarpal region and 2B for the metatarsal region, while the CSA of AIL-SDFT was highest at level 1B. Upon comparing the metacarpal and metatarsal regions, the CSA of SDFT and DDFT was found to be significantly larger at the metatarsal region than at the metacarpal one at certain examination levels. The CSA of SL was significantly larger at the metacarpal than the metatarsal region at level 1A and at the metatarsal region at levels 1B and 3A. The CSA of ICL was significantly larger in the metacarpal region than in the metatarsal region from level 1A to level 3A.

Table 1: Mean±SD values of the cross sectional area (CSA) of tendons and ligaments at palmar metacarpal and plantar metatarsal regions in the studied donkeys

		Zones CSA (mm^2)						
Structure	Region	1A	1B	2A	2B	3A	3B	3C
SDFT	Metacarpal	21.79 ± 2.87^{a}	25.65 ± 2.27^{b}	26.29 ± 1.43^{b}	27.1 ± 1.73^{b}	26.15 ± 2.14^{b}	34.21 ± 2.49^{c}	55.97 ± 4.34^{d}
	Metatarsal	$41.92\pm2.57^{a*}$	23.55 ± 1.43^{b}	29.14 ± 1.8^{c}	29.21 ± 1.8^{c}	37.76 ± 2.4^{d}	$40.87\pm2.5^{ad*}$	$64.98\pm4.0^{e*}$
DDFT	Metacarpal	40.79 ± 2.94^{a}	34.89 ± 2.72^{b}	27.04 ± 2.46^{c}	35.07 ± 3.31^{b}	37.09 ± 3.40^{ab}	49.06 ± 3.33^{d}	40.27 ± 2.9^{a}
	Metatarsal	45.55 ± 2.77^{a}	$40.79\pm2.56^{b*}$	$38.14\pm2.4^{b*}$	37.81 ± 2.5^{b}	33.14 ± 2.1^{c}	$70.50\pm4.14^{d*}$	$52.8475\pm3.2^{e*}$
SL	Metacarpal	$107.47\pm8.03^{ab*}$	$91.11\pm5.56^{c*}$	100.37 ± 5.35^{a}	80.98 ± 4.79^{c}	$95.03\pm4.88^{ac*}$	112.72 ± 5.86^{b}	N/A
	Metatarsal	68.5 ± 4.28^{a}	106.2 ± 6.5^{b}	88.58 ± 6.05^{c}	91.59 ± 5.18^{c}	130.2 ± 6.2^{d}	115.57 ± 7.23^{b}	N/A
ICL	Metacarpal	$31.37\pm1.83^{a*}$	$32.82\pm2.43^{a*}$	$25.96\pm2.24^{b*}$	$15.97\pm1.95^{c*}$	$19.06\pm1.71^{d*}$	N/A	N/A
	Metatarsal	17.375 ± 1.11^{a}	21.47 ± 1.37^{b}	21.19 ± 1.27^{b}	26.23 ± 1.5^{c}	15.62 ± 1.5^{a}	N/A	N/A
AIL-SDFT	Metacarpal	12.10 ± 0.88^{a}	15.17 ± 1.83^{b}	10.93 ± 1.34^{a}	9.12 ± 0.71^{c}	N/A	N/A	N/A
	Metatarsal	N/A	N/A	N/A	N/A	N/A	N/A	N/A

Within the same row: values with different superscripts are significantly different. * Values are significantly different at this level for the same structure among metacarpal and metatarsal regions. A p-value of less than 0.05 was considered statistically significant. SDFT: Superficial digital flexor tendon, DDFT: Deep digital flexor tendon, SL: Suspensory ligament, ICL: Inferior check ligament, and AIL-SDFT: Accessory inferior ligament of superficial digital flexor tendon. N/A: Not applicable

Discussion

The ultrasonographic diagnosis of tendon and ligament injuries depends on changes in shape, echogenicity, size, and fiber pattern (Tsukiyama *et al*., 1996; Pickersgill *et al*., 2001; Davis *et al*., 2006). Accordingly, these variables were established for the examined tendons and ligaments. For complete evaluation, the scanning technique was conducted in transverse planes to determine the normal ultrasonographic appearance and dimensions of tendons and ligaments. The longitudinal plane was used to observe the normal fiber alignment. Craychee (1995) previously employed a similar examination technique in horses.

Tendons and ligaments can be measured in centimeters from a fixed reference point like the accessory carpal bone, point of hock proximally, and ergot distally, thus facilitating the comparison with opposite sides (Smith and Cauvin, 2014). In the current study, the palmar/plantar aspect of the cannon region (metacarpus/metatarsus areas) was divided into seven sequential levels using accessory carpal bone in the forelimb and point of hock in the hind limb as the proximal reference point and the point of ergot as a distal reference point. A similar model was previously utilized in ultrasonographic studies of horses' (Smith *et al*., 1994; ÇLelimli *et al*., 2004; Padaliya *et al*., 2015) and donkeys' distal extremity (Nazem *et al*., 2015; Parés-Casanova, 2021).

In the study reported here, an ultrasonographic scan at the palmar metacarpal region revealed different tendinous and ligamentous structures arranged in the following order: SDFT, DDFT, AIL-SDFT, ICL, and SL. These structures were evident at the first examination level (starting 4 cm below the accessory carpal bone). Conversely, a prior investigation on donkeys revealed no discernible structures at the same level (Nazem *et al*., 2015). This finding can be attributed to the different range of transducer frequency in the current study (10-18 MHZ) compared to the study of Nazem *et al*. (2015) (5-7MHZ).

SDFT, DDFT, and SL were imaged throughout the length of the metacarpal region. However, AIL-SDFT was only present at the first four examination levels. Furthermore, the ICL was only observed as a solitary structure up to level 3A. Nevertheless, it merged with the DDFT in subsequent examination levels (from level 3B to level 3C). In horses, ICL has been reported to be fused with DDFT just below the mid-metacarpal region (Craychee, 1995; Reef, 1998), which could denote a difference in the site of termination of this structure among horses and donkeys.

The third structure to be visualized was the accessory inferior ligament of the superficial digital flexor tendon (AIL-SDFT) that was imaged as an hourglass-shaped structure dorsal to the SDFT and dorsomedial to DDFT from level 1A and distally until level 2B. Nazem *et al*. (2015) reported a similar finding, although it was only observed at level 1B and referred to as the second accessory ligament of the superficial digital flexor tendon. In the present study, we opted for different nomenclatures to provide a more detailed description of the location of this structure. However, it remains imperative to conduct a histomorphological study to confirm the ligamentous nature of the observed structure.

Unlike different structures in the palmar metacarpal region, SL displayed heterogeneous echogenicity. Comparable findings were demonstrated in horses and donkeys (Gillis *et al*., 1995; Maoudifard, 2008; Nazem *et al*., 2015). The heterogeneity of SL can be attributed to its composition of muscle tissue, connective tissue, fat, and ligamentous fibers (Reef, 1998; Caniglia *et al*., 2012). The present study observed that SL exhibited varying levels of heterogeneity across different examination levels. Histomorphological studies are required to investigate this finding deeply.

By conducting a longitudinal scan along the entire length of the metacarpus, it was observed that both SDFT and DDFT exhibited a uniform linear fiber alignment parallel to the longitudinal axis of MCIII. Similar findings were previously detected in horses and donkeys (Gillis *et al*., 1995; Nazem *et al*., 2015). In contrast, the scanned ligaments (SL, ICL, and AIL-SDFT) did not exhibit uniform fiber alignment patterns along all examination levels. However, they exhibited linear and parallel alignment at specific levels, whereas, at other levels, they displayed crimp (waving) patterns or definite patterns. This can be attributed to the pattern of collagen fiber arrangement. According to reports, tendons have collagen fibers arranged in a strict parallel pattern. In contrast, ligaments have collagen fibers arranged more randomly and with fewer mature cross-links to accommodate multi-axial loading (Dahlgren, 2007). The crimp pattern observed in the scanned ligaments serves as a functional explanation, acting as a buffer that allows for slight longitudinal elongation without causing fibrous damage. This pattern also provides a mechanism for the control of tension and acts as a shock absorber along the length of the tissue (Viidick, 1972).

Specifically, in the case of SL, at specific examination levels (2A, 2B, 3A, and 3B), the alignment of its fibers exhibited a characteristic crimp pattern that seemed more extensive than in other ligaments. This finding can be partially explained based on the histomorphological study findings of SL in horses. The study revealed the presence of well-demarcated bundles of rounded striated skeletal muscle with an angled orientation of 60-70° with respect to the collagenous fibers (crimp pattern histologically) (Souza *et al*., 2010). A similar detailed study must be conducted on donkeys to further interpret the current findings.

To thoroughly scan all structures in the metatarsal region, a plantaromedial angle of insonation was necessary due to the prominent axially concave head of MTIV (lateral splint bone). This was required for the first two examination levels (level 1A-1B) (Whitcomb, 2004). The same approach was also implemented in a pure Catalan donkey breed (Parés-Casanova and

Junquera-Muñoz, 2021). The present study partially corroborated previous findings, indicating that the plantaromedial angle of insonation was required to obtain a complete scan of all structures at level 1A. In contrast, the traditional angle of insonation was suitable at level 1B. Therefore, we hypothesized that the head of MTIV in the Equus asinus (the subject of the current study) might be less concave and less prominent than in horses or Catalan donkeys. Further detailed studies of the Equus asinus bony skeleton are required to validate this hypothesis.

Transverse scanning of the plantar metatarsal region revealed the presence of some variations in the sonographic characteristics of the scanned structures relative to the palmar metacarpal region. One of these pertained to SDFT, exhibiting different sonographic shapes at two corresponding examination levels (2A and 3A). Another difference was the absence of AIL-SDFT at the plantar metatarsal region. This finding is consistent with the data published in Catalan donkeys (Parés-Casanova and Junquera-Muñoz, 2021). The superficial digital flexor muscle in horses is predominantly tendinous with minimal or no muscle tissue. As a result, there is no superior check ligament in the hind limb, unlike in the forelimbs (Back *et al*., 1995; Schuurman *et al*., 2003). This might also explain the absence of AIL-SDFT in the metatarsus compared to the metacarpus in the current study.

This study noted that plantar ligament was discernible with other scanned structures in the same scan at level 1A (plantaromedial) and 1B (traditional scan) without lateral scanning or using a standoff pad. In contrast, a standoff pad was recommended for horses to widen the ultrasound window to permit imaging of this ligament, and a lateral scan was required to obtain a complete image (Smith and Cauvin, 2022).

In the plantar metatarsal region, DDFT exhibited sonographic shapes that were comparable to those of palmar metacarpal region except at level 1A (it was of cup shape at metatarsal region and of pear shape at metacarpal region) and level 1B (it was of circular shape at metatarsal region and of pear shape at metacarpal region). The ICL also exhibited different shapes at certain examination levels (level 1A) among the metatarsal and metacarpal regions. Furthermore, a significant discovery was made regarding the presence of ICL, which was found in all of the donkeys examined. However, Barone (1999) found that the ICL might not be present in certain horses and donkeys.

The CSA is the most valid and accurate parameter for detecting tendon or ligament injury (Reef, 1998). Further, in ultrasonographic examination, tendon and ligament cross-sectional area measurements can vary substantially within a few centimeters of the examined area (Marneris and Dyson, 2014). Consequently, the current study measured CSA for each structure in every examination zone. For the metacarpal region, the CSA of SDFT ranged from 21.79±2.87 mm² at the most proximal level to 55.97±4.34 mm² at the distal one. Conversely, in the forelimbs of normal Thoroughbred and Standardbred horses, the CSA of the SDFT reached up to 1.2 cm^2 (Gillis *et al*., 1995). This controversy can be explained by the inherent differences between normal Thoroughbred and Standardbred horses and donkeys subjected to the study and by the difference in the growth weight and animal weather height. This hypothesis can be supported by the previously reported variations in measurements of CSA among different breeds of horses (Wood *et al*., 1993; Gillis *et al*., 1995; Gillis, 1997).

At the plantar metatarsal region, the CSA of the DDFT and SDFT was markedly lesser than that described for horses such as Arabians and Thoroughbreds (ÇLelimli *et al*., 2004). This difference agrees that donkeys are less “dynamic” animals than horses. SL’s largest CSA (130.2 ± 6.2 mm²) was observed at level 3A, approximately 10-12 cm distal to the tarsometatarsal joint. On the contrary, in horses, the largest CSA was more proximally and observed just 2 cm distal to the tarsometatarsal joint (Reef, 1998; Schramme *et al*., 2012). In the present study, along metatarsal examination zones, the CSA of DDFT was mostly larger than that of SDFT. Similarly, in a previously published report on Catalan donkeys, the thickness, another ultrasonographic measurement, was larger for DDFT of the metatarsal region than that of SDFT (Parés-Casanova and Junquera-Muñoz, 2021).

In the present study, the scanned structures’ CSA showed differences between the metatarsal and metacarpal regions. In this regard, the CSA of SDFT and DDFT in the metatarsal region was generally larger than in the metacarpal region at the same levels, with statistically significant differences observed at certain levels. The CSA of the ICL was considerably larger in the metacarpal region compared to the metatarsal region. Consistent with this finding, a previous study observed that in horses, the ICL was slender in the hind limb compared to the fore limb (Barone, 1999). The present study showed a difference in the CSA of SL between metacarpal and metatarsal regions. In this respect, mainly in the proximal examination levels (1A and 2A), its CSA was larger in the metacarpal region than the metatarsal region, and the opposite situation was noted for the lower examination levels (2B, 3A, and 3B). We hypothesized that these variations could be ascribed to disparities in the strain pattern of different structures among the fore and hind limbs and even within the same limb for specific structures. Further studies (biomechanical testing) are necessary to determine the strain pattern of different ligaments and tendons of metacarpal and metatarsal regions in donkeys to either confirm or reject this hypothesis.

The fundamental limitations of this study were the lack of histomorphological studies and biomechanical testing of the examined structures, which would enhance the interpretation of related findings.

In the present study, B-mode ultrasonography revealed shape, echogenicity, echogenic pattern, fiber alignment pattern, and CSA of normal tendons and ligaments at the palmar/plantar aspect of the cannon region of the studied donkeys. Specific differences were

evident in some ultrasonographic features of tendons and ligaments among metacarpal and metatarsal regions. The current study provided a detailed ultrasonographic characterization of normal tendons and ligaments at the palmar/plantar aspect of the cannon region in donkeys (Equus asinus). These data could be a reference guide when cannon region lameness due to tendinopathies and desmopathies is suspected.

Acknowledgements

The authors would like to express their gratitude to the Surgery, Anesthesiology, and Radiology Department staff who contributed to caring for the examined animals.

Conflict of interest

The authors declare that they have no competing interests.

References

Abdel-Hady, AA; Sadan, MA; Metwally, AA and Soliman, AS (2017). Clinico-radiographic studies on the prevalent distal limb affections in working equine at Luxor City. J. Adv. Vet. Res., 7: 24-32.

Assefa, G; Abera, B; Nur, A; Lemma, D; Keno, L; Eticha, E; Chali, G and Hussen, M (2017). The major cause of lameness and associated risk factors in working donkey in and around Hawassa town, Ethiopia. J. Vet. Sci. Technol., 8: 427.

Back, W; Schamhardt, H; Hartman, W and Barneveld, A (1995). Kinematic differences between the distal portions of the forelimbs and hind limbs of horses at the trot. Am. J. Vet. Res., 56: 1522-1528.

Barone, R (1999). Comparative anatomy of domestic mammals. Osteology. Vigot Frères, Paris. 1: 222.

Caniglia, C; Schramme, M and Smith, R (2012). The effect of intralesional injection of bone marrow derived mesenchymal stem cells and bone marrow supernatant on collagen fibril size in a surgical model of equine superficial digital flexor tendonitis. Equine Vet. J., 44: 587-593.

Carnicer, D; Coudry, V and Denoix, JM (2013). Ultrasonographic examination of the palmar aspect of the pastern of the horse: sesamoidean ligaments. Equine Vet. Educ., 25: 256-263.

ÇLelimli, N; Seyrek-Intas, D and Kaya, M (2004). Morphometric measurements of flexor tendons and ligaments in Arabian horses by ultrasonographic examination and comparison with other breeds. Equine Vet. Educ., 16: 81-85.

Craychee, TJ (1995). Ultrasonographic evaluation of equine musculoskeletal injury. In: Nyland, TG and Mattoon, JS (Eds.), *Veterinary diagnostic ultrasound*. (1st Edn.), Philadelphia, W. B. Saunders. PP: 265-304.

Dahlgren, LA (2007). Pathobiology of tendon and ligament injuries. Clin. Tech. Equine Pract., 6: 168-173.

Davis, C; Ely, E; Verheyen, K; Price, J; Wood, J and Smith, R (2006). The value of ultrasonography in monitoring tendon health in racehorses in training. Paper Presented at the 13th ESVOT Congress held at Munich on 7th-10th September, 2006.

Denoix, JM (1994). Functional anatomy of tendons and ligaments in the distal limbs (manus and pes). Vet. Clin. North Am. Equine Pract., 10: 273-322.

Denoix, JM; Crevier, N and Azevedo, C (1992). Ultrasound examination of the pastern in horses. Paper Presented at the Proceedings of the Annual Convention of the American Association of Equine Practitioners (USA).

Gillis, CL (1997). Rehabilitation of tendon and ligament injuries. Proc. Am. Assoc. Equine Pract., 43: 306-309.

Gillis, C; Sharkey, N; Stover, SM; Pool, RR; Meagher, DM and Willits, N (1995). Ultrasonography as a method to determine tendon cross-sectional area. Am. J. Vet. Res., 56: 1270-1274.

Hall, L; Clarke, K and Trim, C (2001). Principles of sedation, anticholinergic agents and principles of premedication, *Veterinary anaesthesia*. (11th Edn.), England, W. B. Saunders. PP: 84-105.

Kimberly, P and Kidd, JA (2014). Introduction. In: Kidd, JA; Lu, KG and Frazer, ML (Eds.), *Atlas of equine ultrasonography*. (1st Edn.), New York City, United States, John Wiley & Sons. PP: 1-22.

Maoudifard, M (2008). Principles of ultrasonography of tendons and ligaments in the horse. Iran J. Vet. Surg., 2: 72-81.

Marneris, D and Dyson, S (2014). Clinical features, diagnostic imaging findings and concurrent injuries in 71 sports horses with suspensory branch injuries. Equine Vet. Educ., 26: 312-321.

Nazem, MN; Sajjadian, SM; Vosough, D and Mirzaesmaeili, A (2015). Topographic description of metacarpal tendons and ligaments of anatoly donkey by ultrasonography and introducing a new ligament. ASJ., 12: 153-160.

Padaliya, N; Ranpariya, J; Kumar, D; Javia, C and Barvalia, D (2015). Ultrasonographic assessment of the equine palmar tendons. Vetworld. 8: 208-212.

Parés-Casanova, PM and Junquera-Muñoz, L (2021). Ultrasonographic study of the plantar region of the hindlimb in a pure breed Catalan donkey. Bulg. J. Agric. Sci., 27: 604-607.

Pickersgill, CH; Marr, CM and Reid, SW (2001). Repeatability of diagnostic ultrasonography in the assessment of the equine superficial digital flexor tendon. Equine Vet. J., 33: 33-37.

Pilsworth, R and Head, M (2010). Presales radiographic surveys in yearlings 1. Image interpretation and significance of lesions in the fetlock. In Practice. 32: 174-183.

Pritchard, J; Lindberg, A; Main, D and Whay, H (2005). Assessment of the welfare of working horses, mules and donkeys, using health and behaviour parameters. Prev. Vet. Med., 69: 265-283.

Rantanen, N; Jorgensen, J and Genovese, R (2003). Ultrasonographic evaluation of the equine limb: technique. In: Ross, MW and Dyson, SJ (Eds.), *Diagnosis and management of lameness in the horse*. (1st Edn.), Philadelphia, Saunders. PP: 166-188.

Reef, VB (1998). Musculoskeletal ultrasonography. *Equine diagnostic ultrasound*. (1st Edn.), Philadelphia, W.B. Saunders. PP: 39-186.

Rheimer, JM (2010). How to maximize image quality for the sonographic evaluation of the hind proximal suspensory ligament. In Proceedings, 56th AAEP. PP: 239-243.

Salem, M; El-Shafaey, ES; Farag, AM; El-Khodery, S; Al Mohamad, Z and Abass, M (2022). A descriptive study of the carpal joint of healthy donkeys using ultrasonography, computed tomography, and magnetic resonance imaging. Vet. Sci., 9: 249.

Salem, M; El-Shafaey, ES; Mosbah, E and Zaghloul, A

(2019). Ultrasonographic, computed tomographic, and magnetic resonance imaging of the normal donkeys (*Equus asinus*) digit. J. Equine Vet. Sci., 74: 68-83.

Schade, J; de Souza, AF; Vincensi, LC; Müller, TR and Fonteque, JH (2021). Clinical and ultrasonographic findings of the digital flexor tendons and ligaments of the metacarpal/metatarsal region in gaited horses. Pferdeheilkunde. 37: 597-604.

Schramme, M; Josson, A and Linder, K (2012). Characterization of the origin and body of the normal equine rear suspensory ligament using ultrasonography, magnetic resonance imaging, and histology. Vet. Radiol. Ultrasound. 53: 318-328.

Schuurman, SO; Kersten, W and Weijs, WA (2003). The equine hind limb is actively stabilized during standing. J. Anat., 202: 355-362.

Smith, KW and Cauvin, RJ (2014). Ultrasonography of the metacarpus and metatarsus. In: Kidd, JA; Lu, KG and Frazer, ML (Eds.), *Atlas of equine ultrasonography*. (1st Edn.), New York City, United States, John Wiley & Sons. PP: 84-116.

Smith, RKW and Cauvin, ERJ (2022). Ultrasonography of the metacarpus and metatarsus. In: Kidd, JA; Lu, KG and Frazer, ML (Eds.), *Atlas of equine ultrasonography*. (2nd Edn.), New York City, United States, John Wiley & Sons. PP: 85-127.

Smith, RK; Jones, R and Webbon, PM (1994). The cross-sectional areas of normal equine digital flexor tendons determined ultrasonographically. Equine Vet. J., 26: 460-465.

Souza, M; van Weeren, PR; Van Schie, H and Van De Lest, C (2010). Regional differences in biochemical, bio-mechanical and histomorphological characteristics of the equine suspensory ligament. Equine Vet. J., 42: 611-620.

Spinella, G; Valentini, S; Pitti, L; Carrillo, JM; Rubio, M; Sopena, J; Santana, A and Vilar, JM (2018). Ultra-sonographic evaluation of cross-sectional area of tarsal ligaments in Standardbred Trotter Horses. J. Appl. Anim. Res., 46: 915-919.

Tsukiyama, K; Acorda, J and Yamada, H (1996). Evaluation of superficial digital flexor tendinitis in racing horses through grey scale histogram analysis of tendon ultrasonograms. Vet. Radiol. Ultrasound. 37: 46-50.

Uerpmann, HP (1991). Equus africanus in Arabia. Equids in the Ancient World. 2: 12-33.

Usman, S; Disassa, H; Kabeta, T; Zenebe, T and Kebede, G (2015). Health and welfare related assessment of working equine in and Around Batu Town, East Shoa, Central Ethiopia. Nat. Sci., 13: 1-8.

Viidick, A (1972). Simultaneous mechanical and light microscopic studies of collagen fibers. Z. Anat. Entwicklungsgesh. 136: 204-212.

Whitcomb, MB (2004). Ultrasonographic evaluation of the metacarpus, metatarsus, and pastern. Clin. Tech. Equine Pract., 3: 238-255.

Wood, AK; Sehgal, CM and Polansky, M (1993). Sonographic brightness of the flexor tendons and ligaments in the metacarpal region of horses. Am. J. Vet. Res., 54: 1969-1974.